Supplementary Materials

Nakano et al. Targeted disruption of *Pparγ1* promotes trophoblast endoreduplication in murine placenta

Supplementary Methods

Mice

Pregnant C57BL/6J mice were purchased from Clea (Tokyo, Japan) at 7 or 10 days post-coitum (dpc). The mice were sacrificed at 10, 12, 14, 16, and 18 dpc under deep anesthesia with isoflurane to obtain the conceptuses. The placentas and fetuses were separated, except for 10 dpc, and they were frozen immediately. The tissues were used to estimate gene expression of *Pparγ1*, *Pparγ1sv*, and *Pparγ2* with reverse transcript quantitative PCR (RT-qPCR) analysis.

Genotyping

For PCR genotyping, a KOD FX Neo kit (TOYOBO life Science, Tokyo, Japan) was used. DNA was obtained from proteinase K-digested tail and yolk sac biopsies from adult mice and fetuses, respectively. Primers used were as follows: F1: 5'-ATT CGC CTT CAT AAC ATT CT-3'; F2: 5'-TGG TCT GGC TGT GTT CTT GTA CTG-3'; F3: 5'-GTA ACT GAC AGC CTA ACC CT-3'; F4: 5'-TGT GCT CGA CGT TGT CAC TGA A-3'; R1: 5'-TGC TGC TCC AAA TGC TCG TAG TAT C-3'; R2: 5'-CCT CAG ACC GAT GTC CAT G-3'; R3: 5'-CGA GCC CCT CTC TAA ATC TGT-3'.

Scanning electron microscopy

Deparaffinized and hydrated thin placental sections were treated with TI blue (Nisshin EM Co., Ltd., Tokyo, Japan) and scanned using a Miniscope® TM3000.

RNA-sequence

The RNA library was prepared from high-quality RNA depleted of rRNA. Following adaptor ligation, the resulting DNA was amplified by PCR for 12 cycles and purified. Libraries were quantified and then used for cluster generation and sequencing. For sequencing details, see below.,

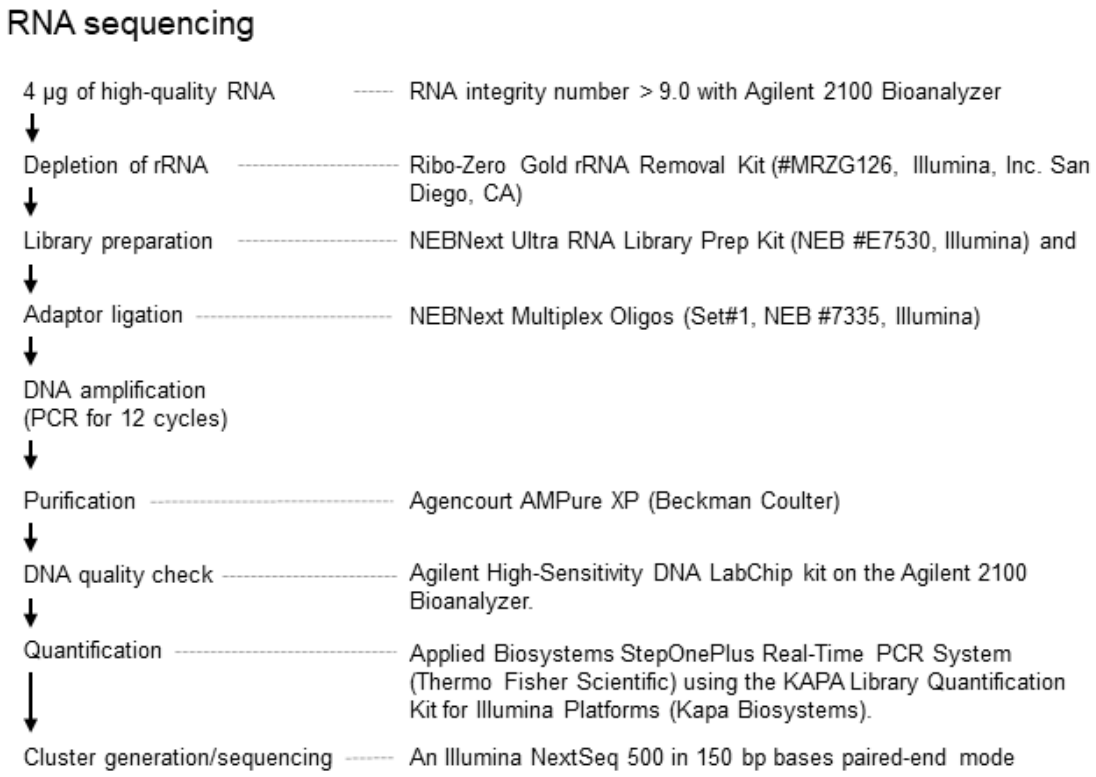

Analysis of RNA-sequence data

Low-quality bases were removed from the reads above, and the resulting trimmed sequencing reads were aggregated into a rRNA reference to remove rRNA reads. Then, the clean reads were mapped to the grcm38_snp_tran reference genome and sorted. Gene expression levels were measured with FPKM (fragments per kilobase of exon per million reads mapped) calculated using R package Ballgown. The readcounts were calculated by using HTseq. *P* values for the difference among genotypes were obtained using the edgeR package (https://bioconductor.org/packages/release/-bioc/html/edgeR.html). DAVID (https://david.ncifcrf.gov/) was used for GO analysis. $p < 0.05$ was considered to be significant in the analyses. For the analysis procedure details, see the flow chart on the next page.

Analysis of RNA-sequence data (*Continued*)

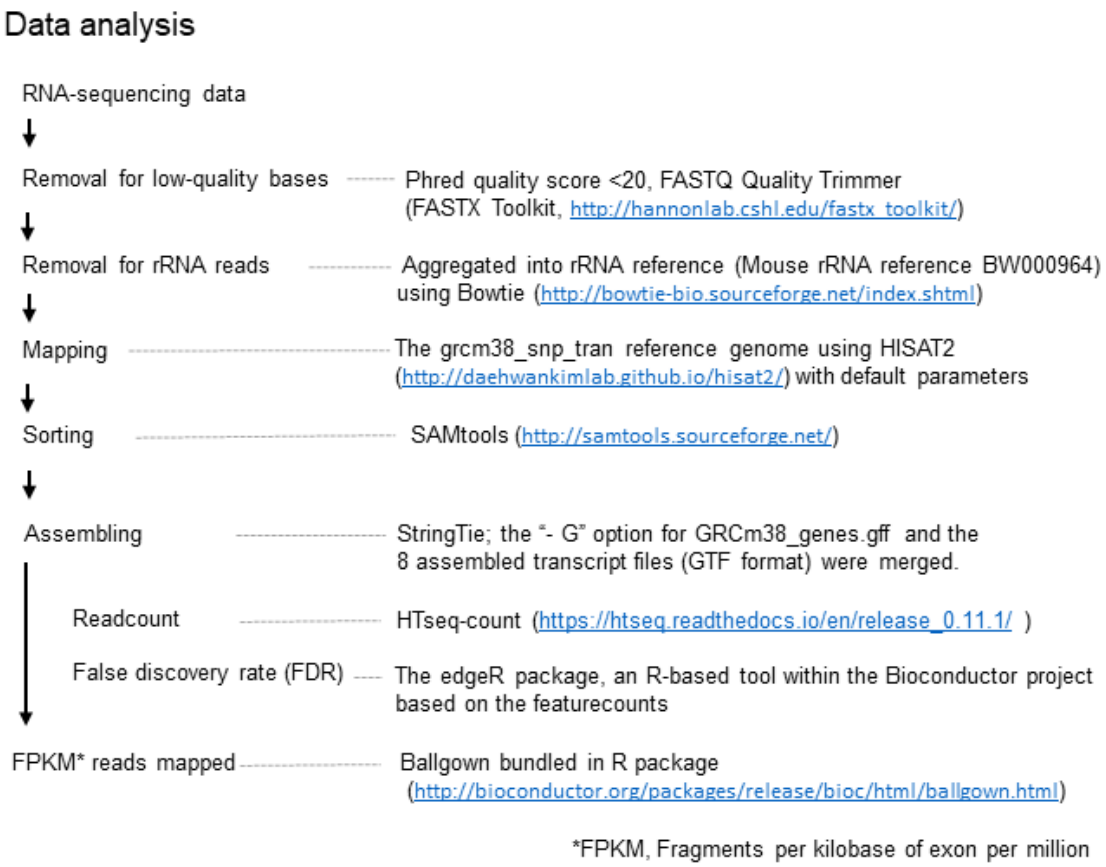

Supplementary figures

Supplementary Figure 1. Exon structure for Pparγ-related genes

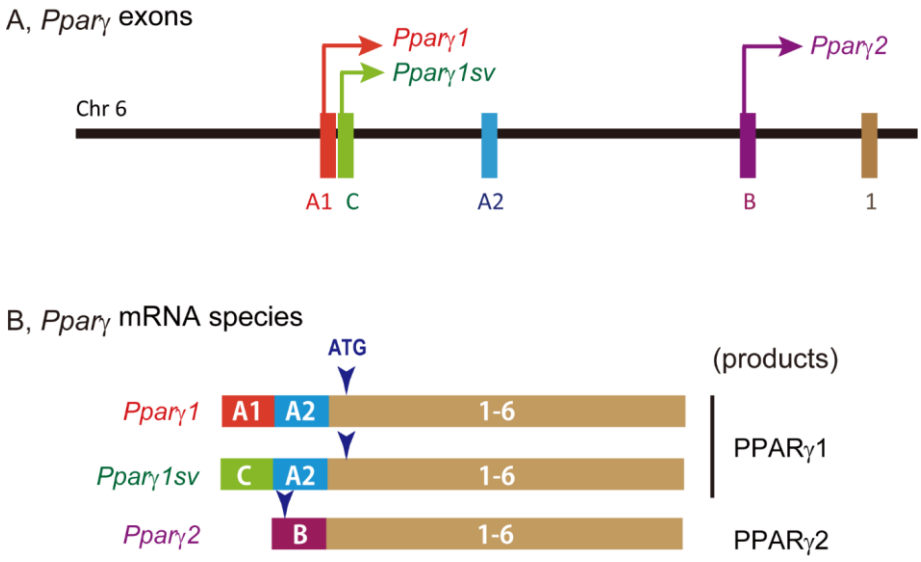

A, Structure of *Pparγ* exons on chromosome (chr) 6. *Pparγ1* and *Pparγ1sv* start at exon A1 and exon C, respectively. *B*, Resulting mRNA structures for *Pparγ* species. Exon A1 and exon C are specific transcripts for *Pparγ1* and *Pparγ1sv*, respectively. Modified from Takenaka Y, Inoue I, Nakano T, Shinoda Y, Ikeda M, Awata T, Katayama S (2013), A Novel Splicing Variant of Peroxisome Proliferator-Activated Receptor-γ (*Pparγ1sv)* Cooperatively Regulates Adipocyte Differentiation with *Pparγ2*. PLoS ONE 8:e65583 [This paper was published under a CC BY license].

Supplementary Figure 2. CAGE data for Pparγ1 and Pparγ1sv in the placenta

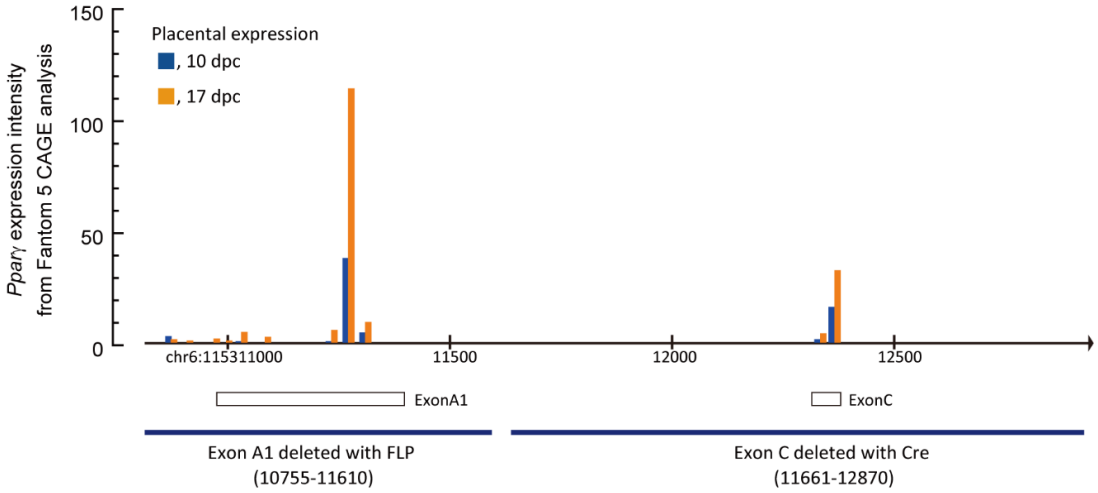

The X-axis shows the genome region that includes exon A1 and exon C on chromosome (chr) 6 refers the mm9 database. The Y-axis shows the transcription start sites and their density for *Ppar*γ expression at 10 dpc (*yellow*) and 17 dpc (*blue*) in mice obtained at the FANTOM5 mouse promoterome view (http://fantom.gsc.riken.jp/zenbu/ accessed in July, 2019). The boxes under the X-axis indicate the sites of the exons. The blue bars at the bottom indicate sites that were genetically deleted for the development of transgenic mouse lines in the present study.

Supplementary Figure 3. Exon A1- or exon C-specific deletion in the mouse genome

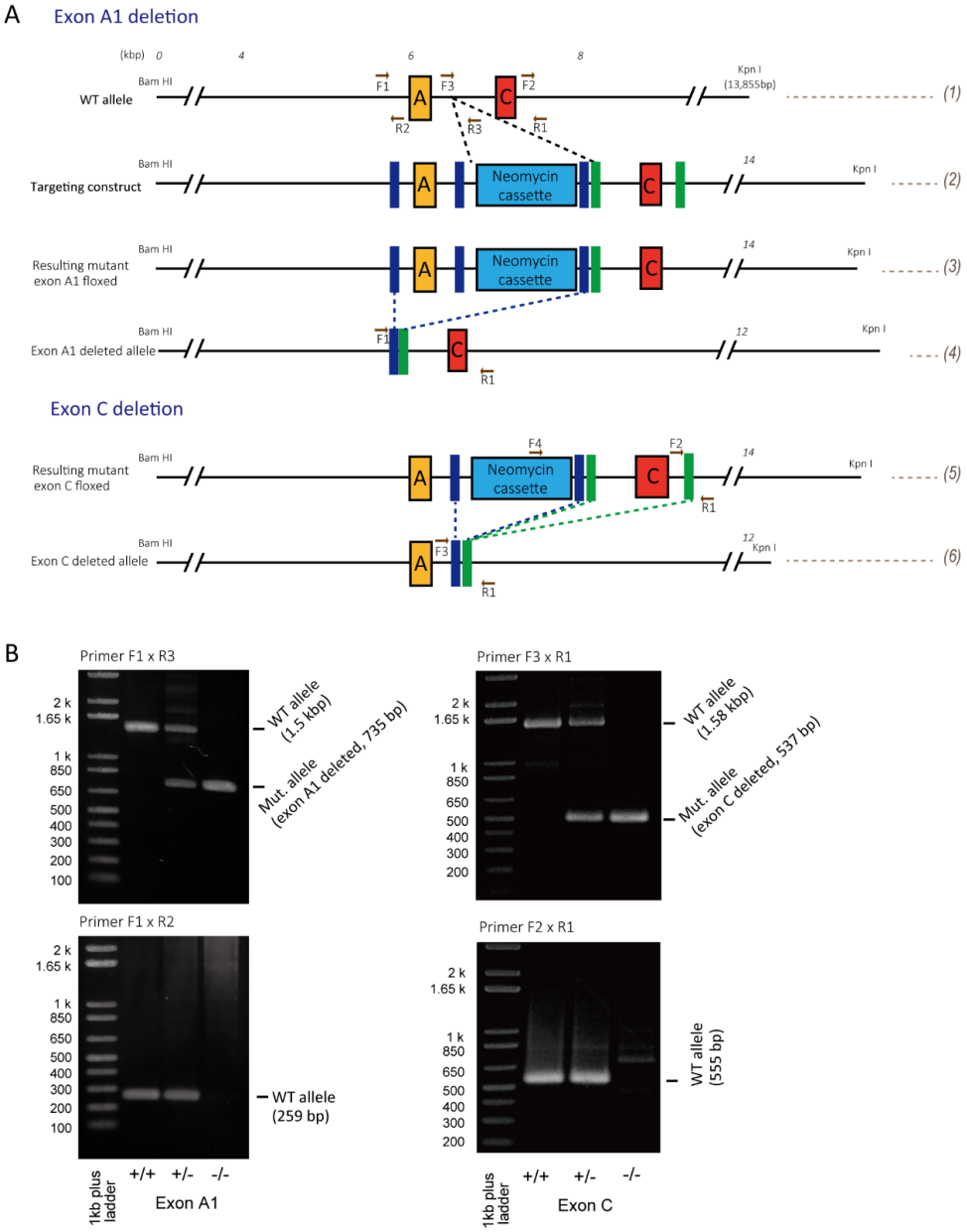

A, Exon A1 and exon C deletion procedures using gene targeting. *(1) WT* allele represents the genomic region containing exon A1 and exon C. *Arrows*, the sites used for priming in PCR. For primers, see Table S2. *(2) Targeting construct* used for homologous recombination with the WT allele. Blue bars, FRT sites; green bars, LoxP sites. *(3)* The resulting mutant allele was floxed for exon A1. Mice with the allele *(3)* were crossed to those with FLP to produce an allele lacking exon A1 *(4)*. *(5,6)* Exon C deletion procedure. *(5)* The resulting mutant allele was floxed for exon C. Mice with the allele *(5)* were crossed to those with Cre to produce allele *(6)* lacking exon C. *B*, Genotyping of resultant mutants with PCR. F1 × R3 and F1 × R2 primer pairs were used for exon A1 deletion allele genotyping. F3 × R1 and F2 × R1 were used for exon C deletion.

Supplementary Figure 4. Pparγ1sv-KO male mice had lower body weight.

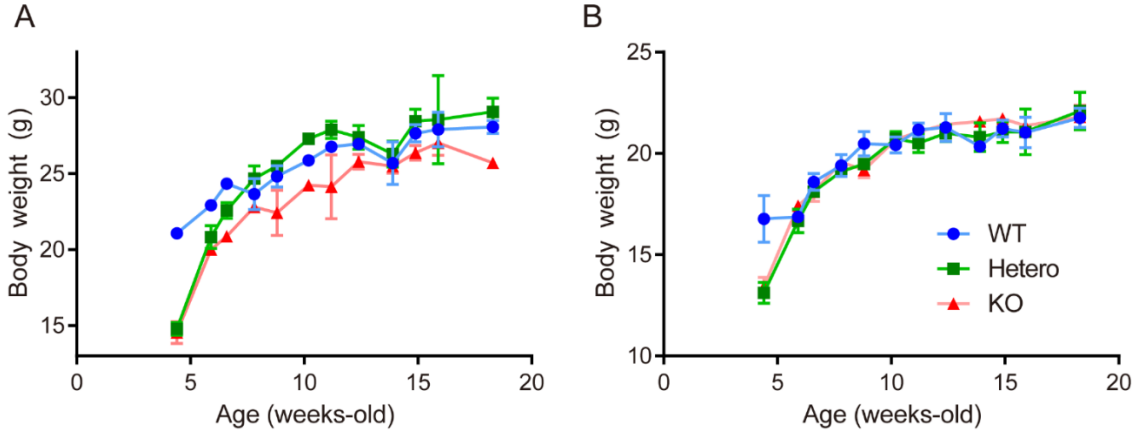

Two-way ANOVA analysis for A and B

Male			Female		
Factors	*F* (DFn, DFd)	*p*-value	Factors	*F* (DFn, DFd)	*p*-value
Interaction	*F* (22, 142) = 2.120	0.005	Interaction	*F* (22, 158) = 1.721	0.03
Age	*F* (11, 142) = 47.83	< 0.0001	Age	*F* (11, 158) = 60.14	< 0.0001
Genotype	*F* (2, 142) = 24.82	< 0.0001	Genotype	*F* (2, 158) = 2.709	0.07

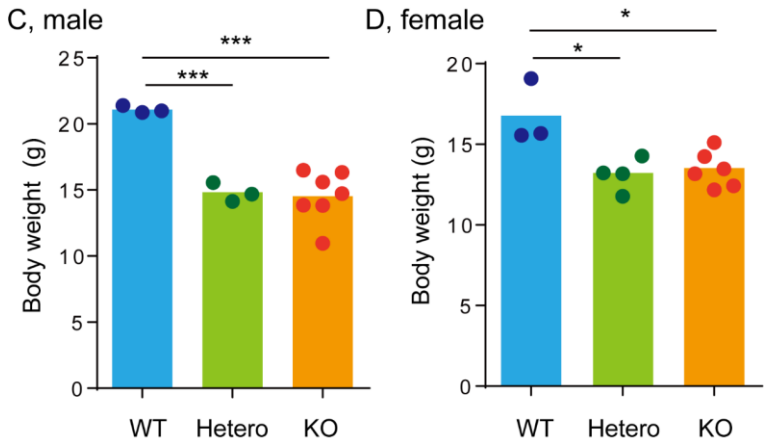

Body weights of *Pparγ1sv*-KO and -Het mice were smaller than the WT counterparts at post-weaning. *A*, In male mice, body weight of KO tended to be smaller than the other counterparts over the time points measured (for genotype, $p < 0.0001$ by two-way ANOVA, see inset). *B*, In female mice, such significant differences were not observed ($p = 0.07$). Female mice showed similar body weight between the genotypes from 5 to 18 weeks old. Body weight was measured occasionally for 13 WT, 16 Het, and 12 KO male mice; for 14 WT, 17 Het, 15 KO female mice. The number of data points ranges from 1 to 13 for each plot. Data are shown as mean and SEM. The data used were not sequential; thus, we did not statistically analyze

the differences between the groups. *C* and *D*, Comparison of body weights from 4 to 5 weeks old showed significantly lower body weights in mice with exon $C^{+/-}$ and exon $C^{-/-}$. Statistical significance was obtained using Students-t test after one-way ANOVA analyses (for male, F (2, 10) = 20.89, p = 0.0003; for female, F (2, 10) = 8.070, p = 0.008). *, $p < 0.05$; ****, $p < 0.0001$.

Supplementary Figure 5. Preliminary examination to detect PPARγ protein using western blotting

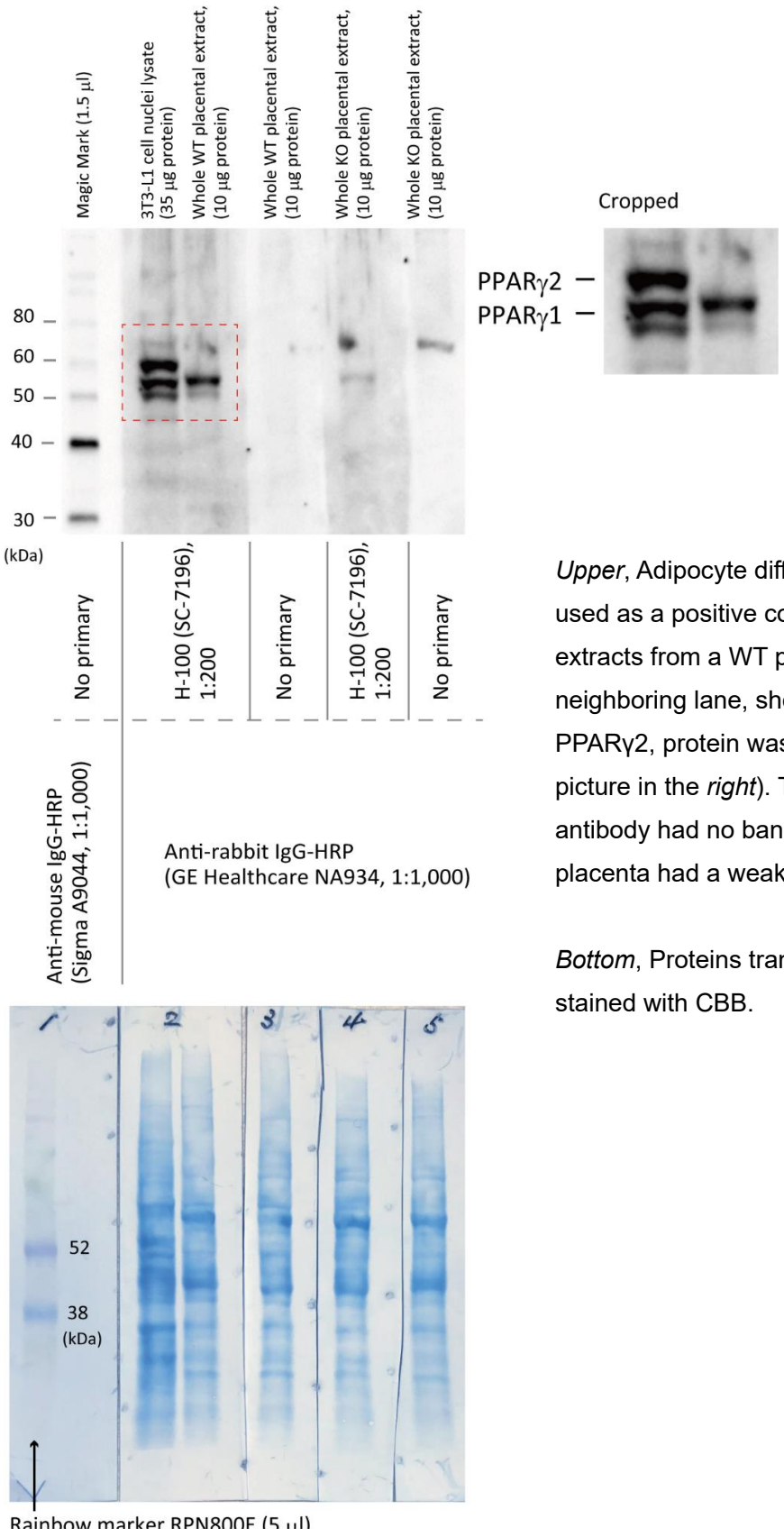

Upper, Adipocyte differentiated 3T3-L1 cells were used as a positive control for PPARγ. Whole protein extracts from a WT placenta was loaded in the neighboring lane, showing that PPARγ1, but not PPARγ2, protein was present (also see the cropped picture in the *right*). The lane with no primary antibody had no bands. The extract from a KO-placenta had a weak PPARγ1 protein band.

Bottom, Proteins transferred to a membrane and stained with CBB.

Supplementary Figure 6. Mice with Pparγ1$^{+/-}$ develop and grow normally.

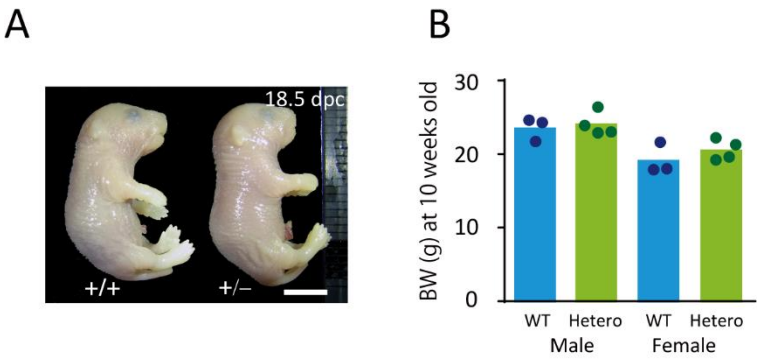

A, No developmental retardation was observed in *Pparγ1*$^{+/-}$ mice.

B, No difference between WT and Het in body weight at 10 weeks old.

Supplementary Figure 7. PPARγ expression in the labyrinth at the 15.5 dpc

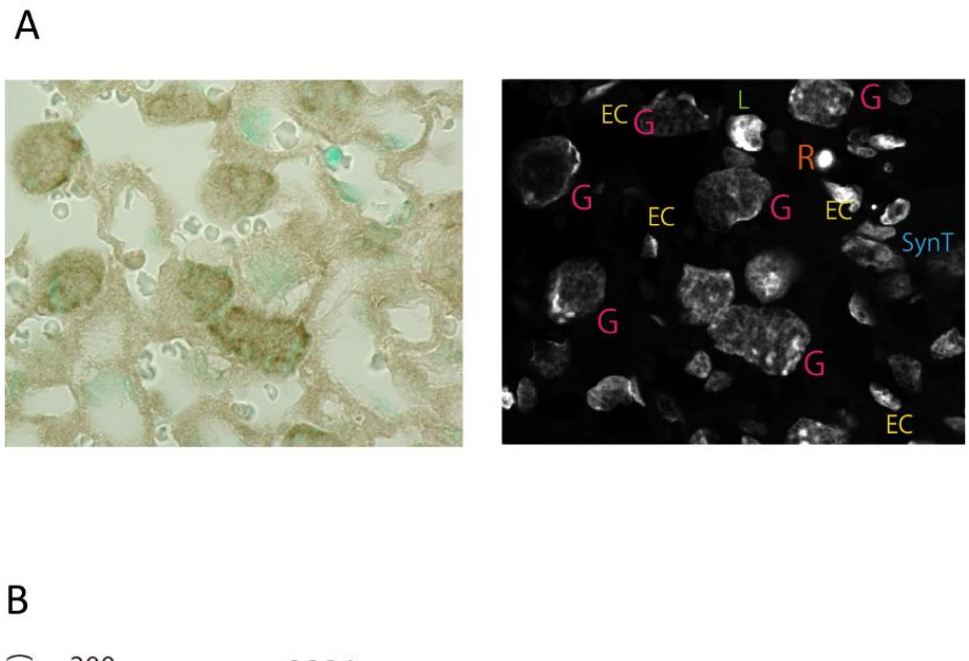

A, *Pparγ1*-WT staining with PPARγ (DAB) and nuclei (methylene blue). *Left*, bright field microscopy; *Right*, methylene blue fluorescence image. G, trophoblast giant cells; EC, endothelial cells; R, red blood cell; SynT, syncytiotrophoblast. *B*, Quantification of DAB intensity. *Pparγ1*-KO placentas were not examined because apparent staining was not observed. WT and heterozygotes were compared using Student's *t*-test. ND, not determined. Bars indicate means.

Supplementary Figure 8. PPARγ expression in other trophoblast giant cells.

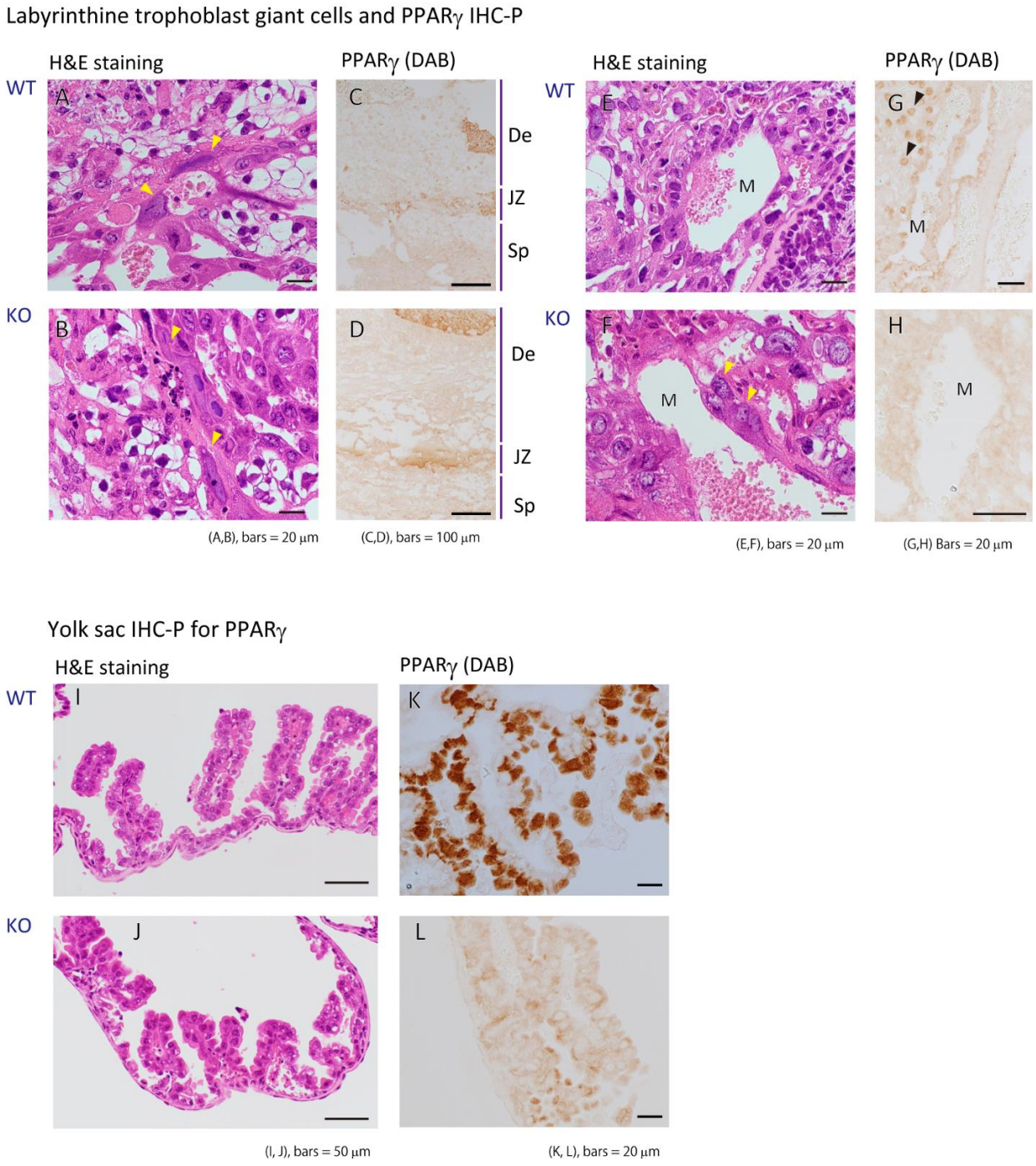

A-H, No apparent PPARγ-immunostaining in parietal (*A-D*) and maternal blood canal-associated (*E-H*) TGCs. Yellow arrow heads in panels *A*, *B*, and *F* indicate TGCs. Black arrow heads in panel G indicate the presence of sinusoidal TGCs in the labyrinth. De, decidua; JZ, junctional zone; Sp, spongiotrophoblast. *I-L*, Histological analyses of yolk sac at 15.5 dpc. *I* and *J*, H&E staining for the yolk sacs. *K* and *L*, PPARγ immunostaining for cuboidal epithelial cells in the yolk sac (*K*). Intensive staining can be seen only in WT, but not KO (*L*). For the discrimination of TGC species, see "Hu D, Cross JC (2010), Development and function of trophoblast giant cells in the rodent placenta. *Int J Dev Biol* 54:341-354."

Supplementary Figure 9. Scanning electron microscopy of the labyrinth zone

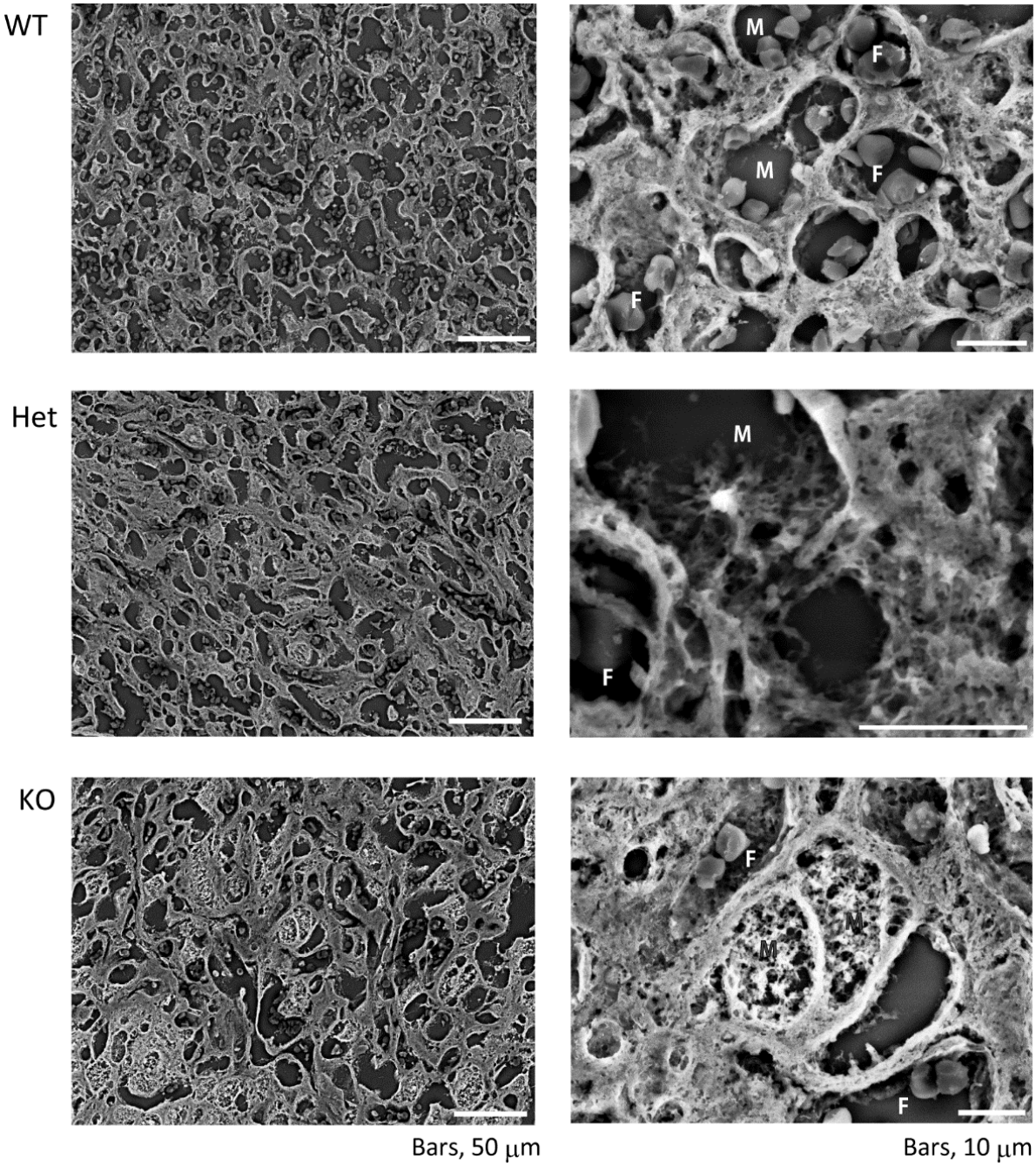

SEM shows that maternal blood sinuses (M) are round and have a smooth surface. Deletion of the *Pparγ1* gene made them squashed and enlarged. The surfaces were coarse, especially in the KO. F, fetal blood capillary.

Supplementary Figure 10.

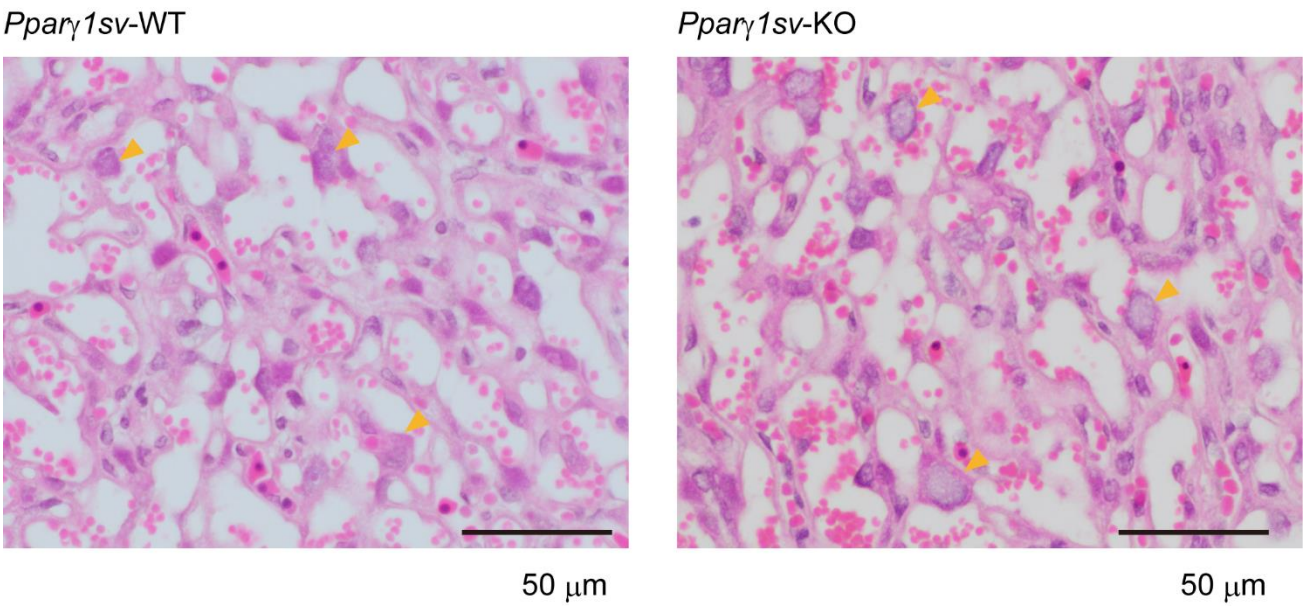

H&E staining of labyrinth in placentas carrying male embryos obtained from pregnant mice at 15.5 dpc. Right and left panels show *Pparγ1sv*-WT, and -KO labyrinths of the placentas, respectively. Arrowheads indicate the nuclei of sinusoidal trophoblast giant cells.

Supplementary Figure 11. Transmission electron microscopy analysis of the labyrinth

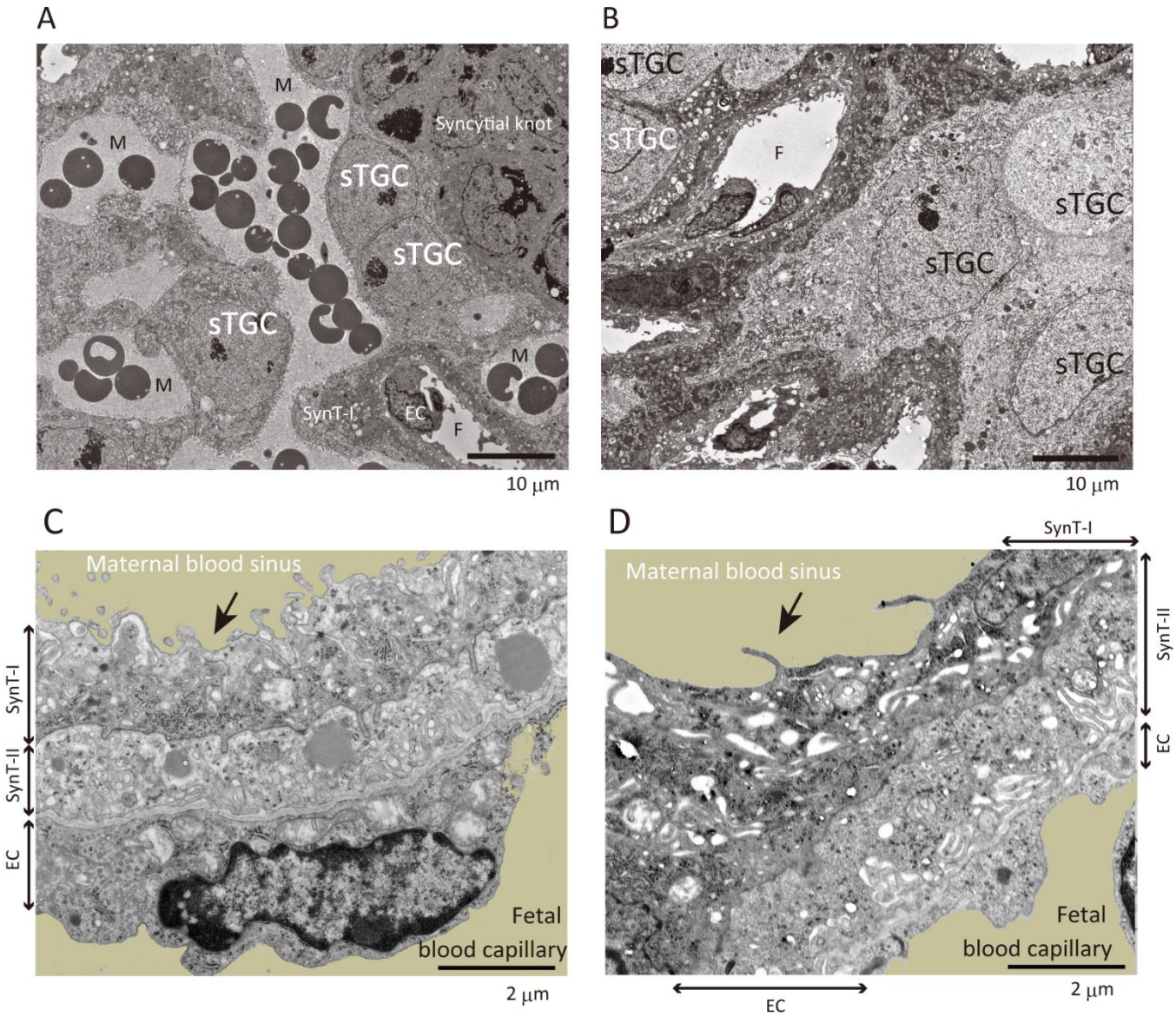

WT on the *left* (*A, C*), KO on the *right* (*B, D*). *A* and *B* show the spatial localization of sinusoidal TGCs (sTGC) in the section. Sinusoidal TGCs were not facing the maternal blood sinus in the KO (*B*). *C* and *D* show feto–maternal interfaces. Poor microvillus development to the KO maternal blood sinus was apparent, as indicated by arrows (*D*). TGC, trophoblast giant cells; M, maternal blood sinus; SynT, syncytiotrophoblast; EC, endothelial cell; F, fetal blood capillary. Bars in *A* and *B*, 10 μm; 2 μm in *C* and *D*.

Supplementary Figure 12. Effect of Pparγ1-deletion on the placental gene expression

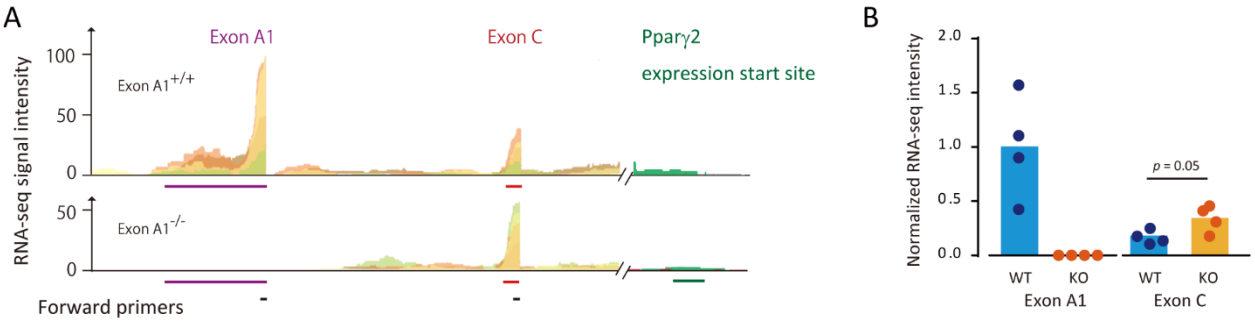

C

GO analysis for placental RNA-sequencing output

GO Term	P-Value
Up-regulated	
Nucleosome assembly	8.0E-16
DNA methylation on cytosine	4.0E-14
Negative regulation of megakaryocyte differentiation	4.2E-06
DNA-templated transcription, initiation	6.1E-05
Cell-cell adhesion	2.6E-04
Negative regulation of transcription from RNA polymerase II promoter	6.4E-04
Membrane raft assembly	6.8E-04
Phosphorylation	9.9E-04
Down-regulated	
Female pregnancy	3.2E-10
Inflammatory response	1.4E-06
Response to hypoxia	2.8E-05
Positive regulation of inflammatory response	1.3E-04
Positive regulation of angiogenesis	1.3E-04
Positive regulation of gene expression	1.4E-04
Positive regulation of cell migration	2.3E-04
Aging	3.1E-04
Axon guidance	5.5E-04
Proteolysis involved in cellular protein catabolic process	6.9E-04
Retrograde protein transport, ER to cytosol	9.3E-04

Supplementary Figure 12 (continued)

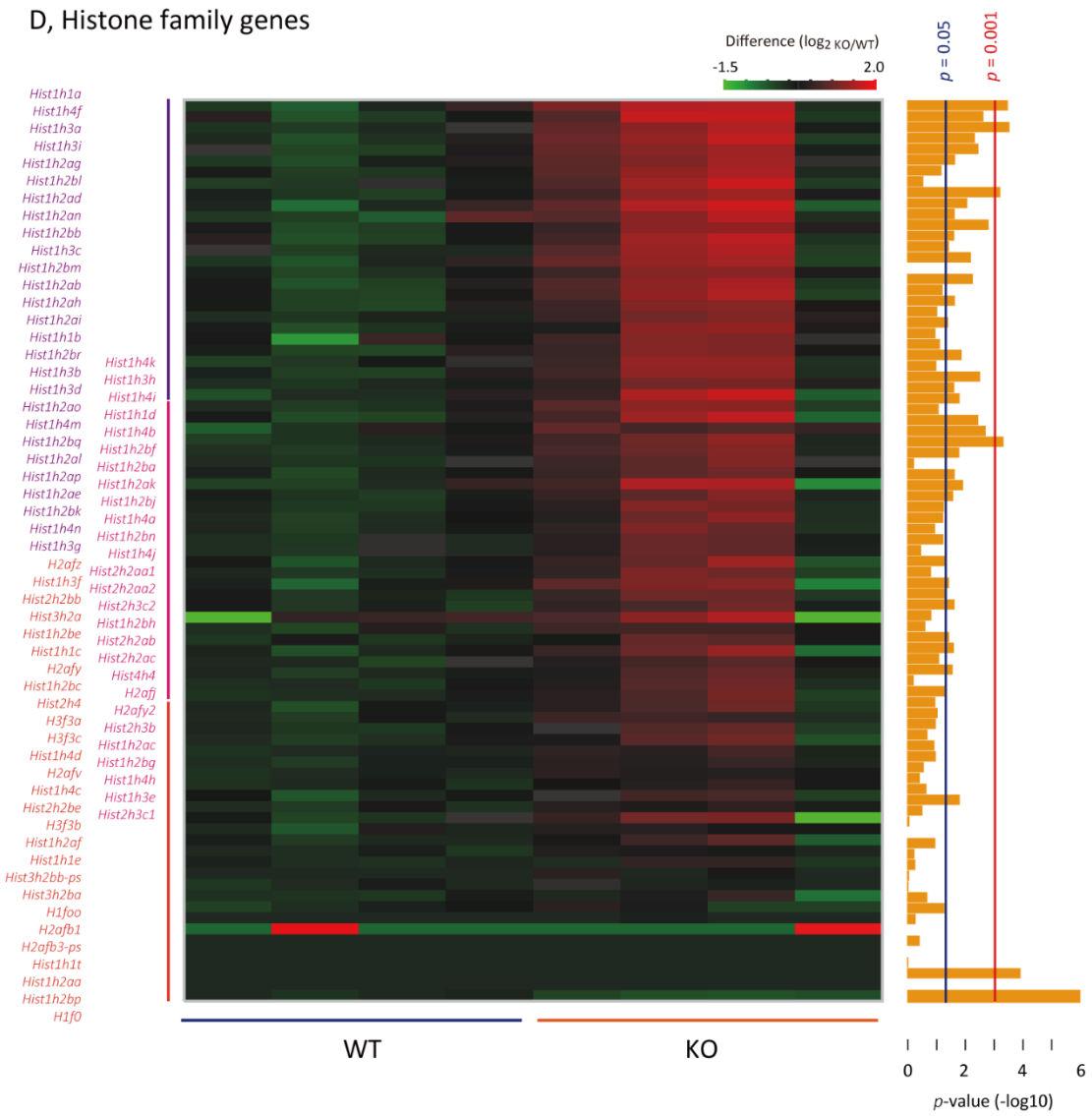

RNA-sequencing analysis reveals endoreduplication signature and pregnancy-related gene expression dysregulation

A, Gene expression of *Ppary* species starting sites (X-axis) and the frequency (Y-axis) are visualized for four replications. Each first exon is indicated with the respective bars. *B*, Comparison of signal intensity using RNA-sequencing between WT and KO. *P* value was obtained using Student's *t*-test. *C*, Tabulated results of gene ontology analysis. *D*, Heatmap presentation for histone-related gene expressions by RNA-sequencing analysis of placentas at 15.5 dpc (n = 4 per genotypes). Log_2 fold changes are pseudocolored with indicated ranges. *p*-values are converted to common logarithm and shown as bar length on the *left* as log_{10} *p*-values.

Supplementary Figure 13

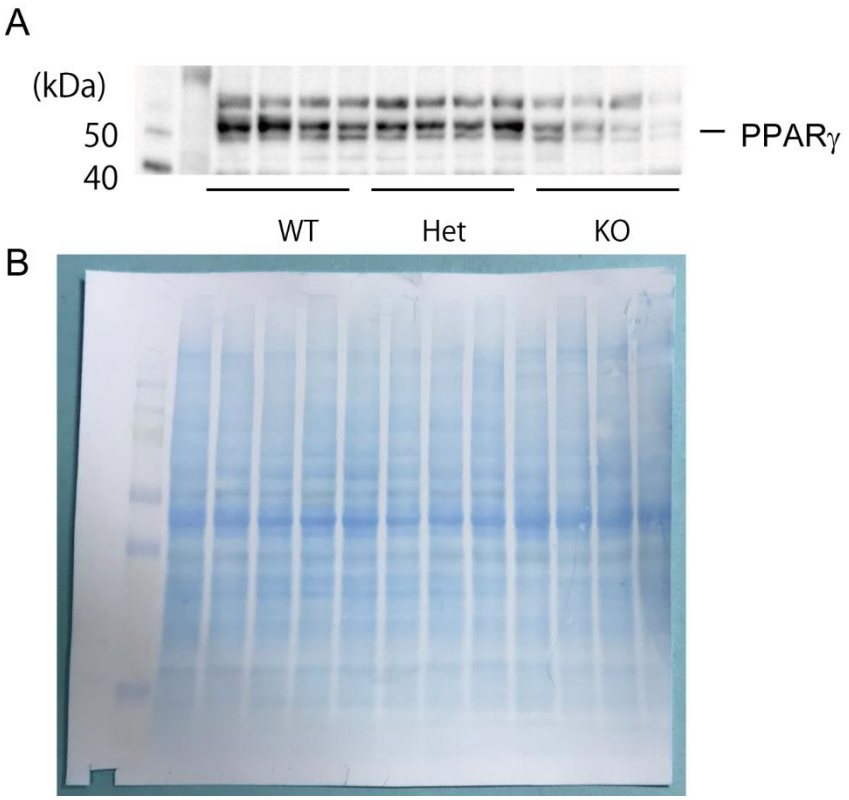

A, Western blotting image shown in Figure 2 (placental PPARγ abundance).

B, Coomassie brilliant blue-stained membrane used in *A*.

Supplementary Tables

Supplementary Table 1.

Genotyping of adult mice from exon C-deletion heterozygous parents (Backcrossed onto B6 ; N=5)

		Genotype			
Sex	No. of mice	+/+	+/-	-/-	*p*-value
Male	82	32	39	11	0.004
Female	91	25	47	19	0.64
Total	173	57	86	30	0.015

p = Hardy-Weinberg's law test

Supplementary Table 2.

Genotyping of adult mice from exon C-deletion heterozygous parents (before backcrossing)

		Genotype			
Sex	No. of mice	+/+	+/-	-/-	*p*-value
Male	35	19	16	0	< 0.001
Female	51	23	29	5	0.003
Total	86	42	45	5	< 0.001

p = Hardy–Weinberg's law test

Table S3. Materials used

Category	Material	Provider	Identifier
Mice and transgenic lines			
Mouse	C57BL/6J	Clea (Tokyo, Japan)	N/A
Vector	FRT-PGK-gb2-neo-FRTloxP	Gene Bridges GmbH, Heidelberg, Germany	A004
Mouse	B6;CBA-Tg(CAG-Cre)47Imeg	Center for Animal Resources and Development, Kumamoto Univ., Kumamoto, Jap	CARD ID.272
Mouse	B6;D2-Tg(CAG-Flp)18Imeg	Center for Animal Resources and Development, Kumamoto Univ., Kumamoto, Jap	CARD ID.265
Instrument	Stereomicroscope	Nikon	SMZ745T with DS-L3 camera
Quantitative RT-PCR			
Reagent	SV Total RNA Isolation System	Promega, Japan (https://www.promega.jp/)	cat.no. Z3100
Reagent	SuperScript IV VILO Master Mix	ThermoFisher Scientific(https://www.thermofisher.com/jp/ja/home.html)	cat.no. 11756050
Reagent	THUNDERBIRD® SYBR qPCR mix	TOYOBO, http://lifescience.toyobo.co.jp/	QPS-201
Instrument	Real-Time PCR System	ThermoFisher Scientific(https://www.thermofisher.com/jp/ja/home.html)	QuantStudio™12K Flex
Western blotting			
Material	Polyvinylidene difluoride membranes (PVDF)/Immunobilon®-P	GE Healthcare	IPVH00010
Antibody	Anti-PPARγ polyclonal antibody (1:1,000)	Santa Cruz	SC-7196 (H-100)
Antibody	Horseradish peroxidase-conjugated anti-rabbit IgG antibody (1:1,000)	GE Healthcare	NA934
Antibody	Horseradish peroxidase-conjugated anti-mouse IgG antibody (1:1,000)	Sigma-Aldrich	A9044
Reagent	ECL Prime™, Western Blotting Detection Reagents	GE Healthcare	RPN2232
Reagent	MagicMark™ XP Western Protein Standard	ThermoFisher Scientific	LC5602
Instrument	Luminescence imager	Bio-Rad laboratories	ChemiDoc™ MP system
Histology			
Instrument	Light microscopy	OLYMPUS Corp	BX53 with DP27 digital camera
Instrument	All-in-one fluorescent microscope	Keyence	BZ-X700
Immunohistochemistry			
Reagent	Vector® M.O.M.™ Immunodetection Peroxidase Kit	Vector laboratories Inc.	PK-2200
Antibody	Anti-PPARγ monoclonal antibody from mouse (1:500)	Perseus Proteomics, Inc.	A3409A
Antibody	Anti-monocarboxylate transporter 1 IgY antibody from Chiken (1:1,000)	Millipore	AB1286-I
Antibody	Alexa Fluor 488-conjugated goat anti-Chicken IgY (1:1,000)	ThermoFsher Scientific	A-11039
Software			
	Photoshop CS5	Adobe Systems	N/A
	ImageJ	https://imagej.nih.gov/ij/	p1.52
	JMP®	SAS Institute Inc.	ver. 13.2.1
	PRISM®	GraphPad Software Inc.	ver 6.07

Table S4. Primers used for quantitative RT-PCR

HGNC symbol	Accession No.	Forward primer (5'-3')	Reverse primer (5'-3')
PPARγ			
Pparγ1	NM_001127330.2	CAGGACTGTGTGACAGACAAGAT	GGCCAGAATGGCATCTCTGTGTCAA
Pparγ1sv	AB644275	GCGCTAAATTCTTCTTAACTC	GGCCAGAATGGCATCTCTGTGTCAA
Pparγ2	NM_011146	GTTATGGGTGAAACTCTGGGAGAT	GGCCAGAATGGCATCTCTGTGTCAA
Cyclins			
Ccna1	NM_001305221.1	ATGAGTTTGTCTACATCACCGACGA	TGATGCACACTCCTTGACGCCTT
Ccna2	NM_009828.3	CGGAGCAAGAAAACCACTGACACC	GCTGCCTCTTCATGTAACCCACT
Ccnb1	NM_172301.3	ATCCTCATTGACTGGCTAATACAGG	TGCAATAAACATGGCCGTTACACC
Ccnb2	NM_007630.2	CTTACACCAGTTCCCAAATCCGAGA	GTCAGCTCCATCAGGTACTTGGCTA
Ccnb3	NM_183015.3	AGTTCCTTCAGAATCCATTGCCACC	CTTGTCATCATTTGAAGCCACCGAT
Ccnd1	NM_007631.2	AGGCGGATGAGAACAAGCAGA	CAGGCTTGACTCCAGAAGGG
Ccnd2	NM_009829.3	GCGTGTTCGTCATCTGCTAGCC	CACCACATGCGTTACAACTATACGG
Ccnd3	NM_007632.2	AGTTGCCAAAACGCCCCAGTACCTT	AATGACCACGGCACCCTTAAGACCC
Ccne1	NM_007633.2	ACTTGGCACAGGACTTCTTTGATCGTT	ACATTCAGCCAGGACACAATGGTCA
Ccne2	NM_001037134.2	ACAAAAGGAAAACAGATACGTGCAT	GCACCATCAGTGACGTAAGCAA
E2F			
E2f1	NM_007891.5	GGGCTGGGTTTGAAACTCTC	GAGTGAACATTCCCTCCAACA
E2f2	NM_177733.7	TCGCTTTACACGCAGACG	GCACATCGCACAATTTGG
E2f6	NM_033270.2	TTCGGAAGAGGCGAGTGTAT	CTTTTCCACCAGTTCGATGC
E2f7	NM_178609.4	CTAAAGTCTGGGTGCCTTGTG	CAGTGTGACCTCATAGTTCATCG
E2f8	NM_001013368.5	GGCCACCAACCATGACTC	GCGACTGGTTGTCCGTTTA
CDK inhibitors			
p19	NM_009878	AGCCTTACTGGGTTACTTGTCAACA	CTGTAGGAGCCCCTTCTTTGTCCA
p21	NM_007669.5	CTGGTTCCTTGCCACTTCTTACCTG	TTACGGTTGAGTCCTAACTGCCAT
p27	NM_009875.4	GTCGCAGAACTTCGAAGAGG	AAACCGAACAAAAGCGAAAC
p57	NM_001161624.1	CTGAAGGACCAGCCTCTCTC	TGCTCTACGCAACCATCTCC
Pregnancy-specific glycoproteins			
Psg16	NM_007676.4	CTCCAATAGTGACACCTAACCCCAA	AAACTGTGAATCAAAACTATCTAGTAGCCA
Psg19	NM_011964.2	TCCAGTGCCACCACATGCTGTC	TGCACGGCCACTGATGATAGACTCT
Psg21	NM_027403.4	TTCTCCCACATCCCCTCTC	GGGGAAAATAATAAGTGGAAGCA
Psg22	NM_001004152.2	CACAGTGGAAGAGAGATATTGTTCA	AAGCCAGAGTCTTTCTCAGTGAC
Psg23	NM_020261.4	GAGCCTGTCCCCGTCAAAGTGT	GAAATGCCTCTGCCCTGCTATAGT
Housekeeping genes			
18s	NR_003278.3	CGGCTACCACATCCAAGGAA	GCTGGAATTACCGCGGCT
HPRT	NM_013556.2	CTATAAGTTCTTTGCTGACCTGCT	ATCATCTCCACCAATAACTTTTATGT